A scanning contact probe for a micro-coordinate measuring machine (CMM)

2010 Meas. Sci. Technol. 21 054002

(http://iopscience.iop.org/0957-0233/21/5/054002)

IOP Publishing Measurement Science and Technology

Meas. Sci. Technol. **21** (2010) 054002 (7pp) doi:10.1088/0957-0233/21/5/054002

A scanning contact probe for a micro-coordinate measuring machine (CMM)

Kuang-Chao Fan[1,3], **Fang Cheng**[1], **Weili Wang**[1], **Yejin Chen**[1] **and Jia-You Lin**[2]

[1] School of Instrument Science and Opto-electric Engineering, Hefei University of Technology, Hefei 230009, People's Republic of China

[2] Department of Mechanical Engineering, National Taiwan University, Taipei 106, Taiwan, Republic of China

E-mail: fan@ntu.edu.tw

Received 21 September 2009, in final form 27 November 2009
Published 23 March 2010
Online at stacks.iop.org/MST/21/054002

Abstract
A new high precision contact scanning probe able to measure miniature components on a micro/nano-coordinate measuring machine (CMM) is proposed. This contact probe is composed of a fiber stylus with a ball tip, a floating plate and focus sensors. The stylus is attached to a floating plate, which is connected to the probe housing via four elastic wires. When the probe tip is touched and then deflected by the workpiece, the wires experience elastic deformations and the four mirrors mounted on the plate will be displaced. These displacements can be detected by four corresponding laser focus probes. To calibrate this touch trigger probe, a double-trigger method is developed for a high-speed approach and a low-speed touch. Experimental results show that the probe has a symmetric contact property in the horizontal XY plane. The contact force is found to be about 109 μN. The standard deviation of the unidirectional touch is less than 10 nm and the pre-travel distance is around 10 nm with a standard deviation of less than 3 nm.

Keywords: scanning contact probe, contact focus, trigger point, pre-travel distance, micro-CMM

(Some figures in this article are in colour only in the electronic version)

1. Introduction

The increasing demand of micro systems in industry for higher measurement accuracy has led to the development of the field of micro/nano-dimensional metrology [1]. Conventional coordinate measuring machines (CMMs), as a versatile dimensional metrology tool, can only measure macro- to meso-scaled parts because of the limitations of the probing system. Several researchers have developed micro- or nano-CMMs that can measure meso- to micro-scaled parts in nanometer resolution, mostly with specially designed probe systems [2–4]. The need of a 3D contact probe, besides non-contact probes, is due to its capability to cope with deep trenches and sidewall measurements. The probing sphere has to be as small as possible. Although a variety of probe systems have been designed, such as silicon-based [5], flexture structure-based [6, 7], and others [8], most of them assemble the stylus by gluing a commercially available micro sphere onto a metal stem. Such a process will inevitably incur the offset error of the sphere to the center of the stylus. Even though many probe systems claim a measurement uncertainty in the range of 20–50 nm, the technique of probe radius compensation has never been mentioned. A scanning contact probe normally consists of an elastic mechanism and several sensors in order to detect the motion of the probe tip in all directions. The contact force has to be small, normally less than 1 mN. The repeatability

---

[3] Author to whom any correspondence should be addressed.

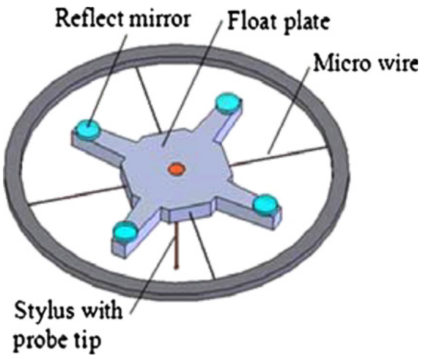

Figure 1. Probe floating mechanism.

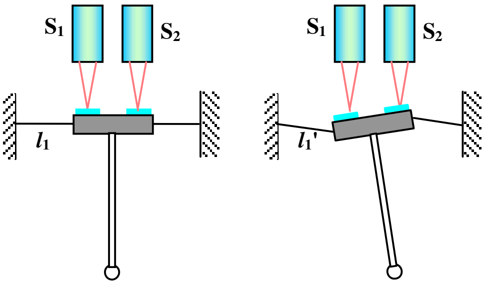

(*a*) (*b*)

Figure 2. (*a*) Probe at rest, (*b*) probe in contact.

has to be very high. The stiffness has to be low and equal in all directions [4, 6, 7].

A new design of the analog tactile probe is proposed in this study. This tactile probe is composed of a monolithic fiber stylus with a ball tip, a floating plate and focus sensors. The ball tip is produced from an optical fiber by a melting and solidification process, which can ensure the required diameter, roundness and center offset within a tolerance of less than 1 μm. The design principle and calibration of the innovative probe will be addressed. Experimental results will also show the capability of contact scanning measurements.

2. Design principle of the probe

Figure 1 shows the mechanism of the proposed contact probe. The glass fiber probe stylus is fixed to a floating plate, which is suspended by four evenly distributed wires connected to the probe housing. The contact force causes a tilt motion of the rigid floating plate while the wires experience elastic deformations. The floating plate has four extended arms. Four mirrors mounted on the respective arms amplify the up/down displacement at each mirror position. These displacements can be detected by four corresponding focus probes (S_1 to S_4) developed in this work. Figure 2 shows one projection view of only S_1 and S_2 effective. The trigger signal of the probe is defined as

$$y = |s_1 - s_2| + |s_3 - s_4|. \qquad (1)$$

Details of the probe components are described below.

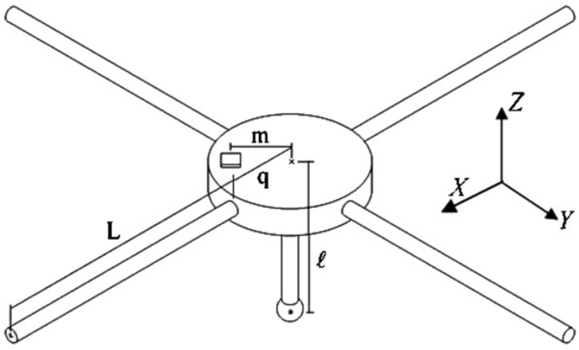

Figure 3. Simplified structure of the floating mechanism.

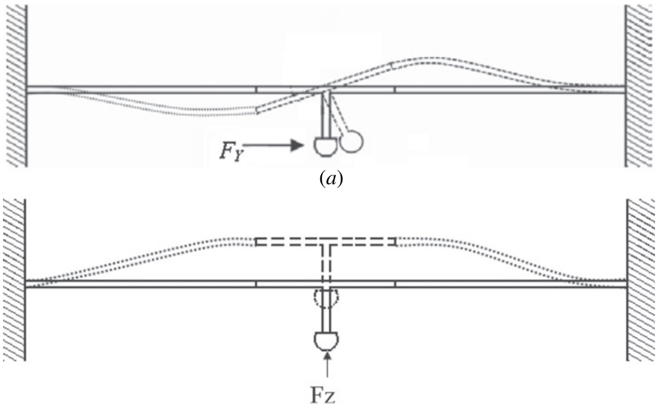

(*a*) (*b*)

Figure 4. Deflection mode under force, (*a*) horizontally and (*b*) vertically.

2.1. *The floating mechanism*

The main task of the floating mechanism is to give the probe a stable rest position and a tilt angle relative to the contact force in three orthogonal directions. The shape and dimension of the floating plate, as well as the length and diameter of the micro wire, are determined according to the selected contact forces. The probing force is normally required to be less than 1 mN. The dimension of the mechanism can be calculated by the finite element method, in order to obtain an optimum geometry. Due to its symmetrical geometry, the force–motion characteristics will be symmetrical in the XY plane.

In order to analyze the response of the displacement to the contact force, the structure of the floating mechanism is illustrated in figure 3, where the floating plate is simplified to a circular form, because the major factor is the deformation of the elastic wire. As shown in figure 4(*a*), when a horizontal force (F_Y) is applied to the ball tip, the two wires located in the same direction will be deflected in the Z-direction in an opposite symmetrical shape. When a vertical force (F_Z) is applied to the ball tip, all wires will be deflected symmetrically in the Z-direction, as shown in figure 4(*b*). From elasticity theory the displacement-to-force relationship can be derived to be

$$\begin{bmatrix} \delta_{X,\mathrm{ball}} \\ \delta_{Y,\mathrm{ball}} \\ \delta_{Z,\mathrm{ball}} \end{bmatrix} = \begin{bmatrix} C_1 & 0 & 0 \\ 0 & C_1 & 0 \\ 0 & 0 & C_2 \end{bmatrix} \begin{bmatrix} F_{X,\mathrm{ball}} \\ F_{Y,\mathrm{ball}} \\ F_{Z,\mathrm{ball}} \end{bmatrix}, \qquad (2)$$

Table 1. The components of the floating mechanism.

Item	Specifications
Elastic wire	Material: copper, $E = 1.1 \times 10^5$ N mm^{-1}, diameter: 0.18 mm, length: 29 mm
Floating plate	Material: copper, base diameter: 14 mm, arm diameter: 43 mm, thickness: 4 mm, weight: 2.5 g
Stylus	Material: glass fiber inserted into a steel needle, length: 5 mm, ball diameter: 313 μm

where $C_1 = \frac{\ell^2 L^3}{8EI\cdot(3q^2+3qL+L^2)}$ and $C_2 = \frac{L^3}{48EI}$. The stiffness of the probe mechanism is the inverse of C in the corresponding direction. The parameters affecting the stiffness are the wire length L, the stylus length l, the plate radius q, the moment of inertia of the wire I and Young's modulus of the wire material E. It is seen that with proper selection of the dimension of the floating mechanism, it is possible to design a probe mechanism of this type with constant stiffness in all directions, i.e. $C_1 = C_2$. In the current design, the components of the floating mechanism are listed in table 1. The stiffness can be calculated as 118 mN mm^{-1} in the X and Y directions, and 11 mN mm^{-1} in the Z direction. Since this is the first model of the probe system, we have not yet achieved a balanced design of the stiffness. This will be our future work.

2.2. *Fabrication of the probe tip*

The probe tip must be spherical with diameters in the range of 500–100 μm, or even less. It is normally made by gluing a micro ball to a micro tungsten wire. The concentricity of the wire to the ball is a problem of the assembly, that will cause a measurement error, because the probe radius has to be compensated for. If the ball is not in line with the stylus center, the amount of radius compensation varies with different angles. A technique of fabricating a monolithic probe stylus by a melting and solidification process of a thin glass fiber in order to form a micro-sphere tip has been developed by the authors [9].

A single mode (SM) glass fiber with a diameter of 125 μm has been selected to produce the ball tip. A glass fiber has sufficient mechanical strength to perform tactile measurements. It can easily be fused in an appropriate heating field. The fiber tip absorbs the arc discharging power and melts instantaneously. Due to the surface tension, the melting part of the fiber starts to gradually form a spherical tip during the solidification. A fiber fusion splicer was the basic apparatus employed in this process, as shown in figure 5. The produced fiber is mounted onto a V-groove and the fiber fixture is precisely positioned by an XY stage. With proper selection of the process parameters in the splicer, the end face of the glass fiber can be melted and formed to a micro sphere due to the surface tension phenomenon. A rotary stage keeps the molten fiber rotating while it solidifies, in order to compensate for gravity.

The optimal process parameters to get a precise probe diameter, the best probe roundness and the smallest center offset are obtained by using Taguchi's method. The image of one of the probes viewed at four different angular positions is shown in figure 6. The corresponding measurement results are summarized in table 2 [10]. All errors can be controlled to within 1 μm.

Table 2. Measurement results of the tip at four different angles (in μm).

Angle of view	0°	90°	180°	270°
Diameter	314.07	313.84	314.05	313.89
Roundness	0.54	0.82	0.37	0.61
Center offset	0.37	0.96	0.28	0.72

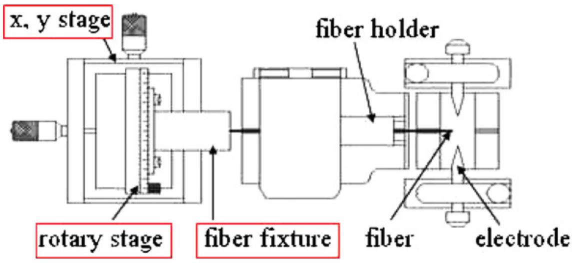

Figure 5. Experimental setup of the fiber tip fabrication.

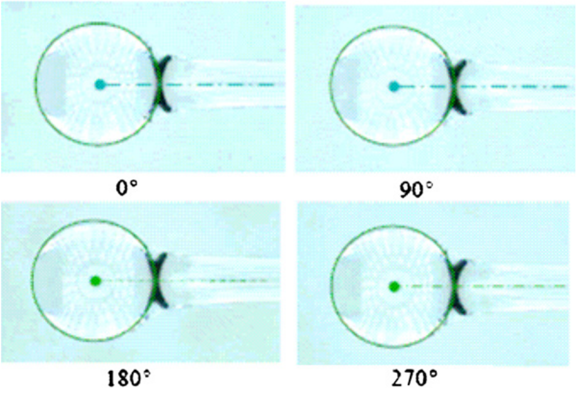

Figure 6. Image of one fiber probe.

It should be noted that the glass fiber stylus and the ball tip may be subject to breakage due to its weak stiffness. In practice, however, the contact force is normally very small and would not cause any damage [11]. In our system, a medical injection steel needle with an inner diameter of 150 μm has been used to insert the stem of the fiber probe, in order to reinforce the stylus. Thus, the situation mentioned will not happen.

2.3. *The focus sensor*

The sensor used in this touch scanning probe is based on a laser focus probe, which is reconfigured from a DVD pickup head. Being a mass production device, the pickup head is cheap but very accurate. The laser focus probe adopts the astigmatism principle, which is explained in the authors'

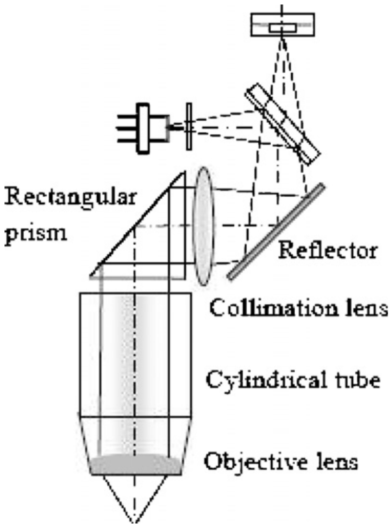

Figure 7. Reconfigured DVD pick-up head.

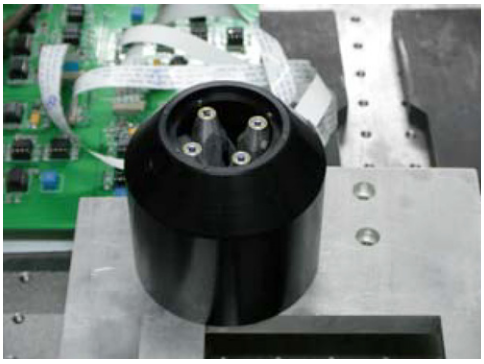

Figure 8. Photo of the probe head.

previous paper [12]. The displacement of the reflection mirror will cause a focus error signal (FES) of the embedded quadrant photodetector. This FES performs an extremely linear curve within the focus range with a resolution of 1 nm [13]. The pickup head is reconfigured by a special design, as shown in figure 7. Figure 8 shows the integration of the four sensors in the probe head without the floating mechanism. Since the FES is the analog signal of the tip displacement during a contact, a combination of four FES signals can reveal the angle and displacement of the probe ball, setting up a contact scanning mode.

3. Calibration of the probe system

As a contact scanning probe, the triggered signal has to be locked before it changes to the analog scanning mode. To ensure the triggered position is precise and repeatable within a nanometer range, the double-trigger method as used in conventional in-cycle gauging of machine tools [14] is adopted for use in the probe system calibration.

3.1. Double-trigger control method

The trigger control requires a very low speed when approaching the workpiece to the probe ball. Normally, the pre-hit position of the probe is far from the touch point. In our experiment, a long-stroke and a nano-positioning co-planar stage [15] has been used to move the workpiece to touch the probe. A fast motion is commanded to the stage before it moves to the vicinity of the probe. A double-trigger method is thus developed, with a high-speed approach and a low-speed touch.

An ultrasonic motor, model HR4 made by Nanomotion Co. [16], is employed to generate three mode motions at different scales. In its ac mode, the HR4 generates a high-speed motion using a neural network PID velocity controller [17]. Then changing to the GATE mode, the HR4 drives the stage in pulses with short steps of 20–50 nm and the average speed is controlled to be 25 μm s^{-1} until the probe ball is touched and deflected. Finally, moving the stage backward in the GATE mode to release the touch and then moving forward again using the dc mode, the HR4 works like a conventional PZT actuator with low speed and nano stepping to perform the second touch. Different calibration programs have been designed by integrating these driving modes.

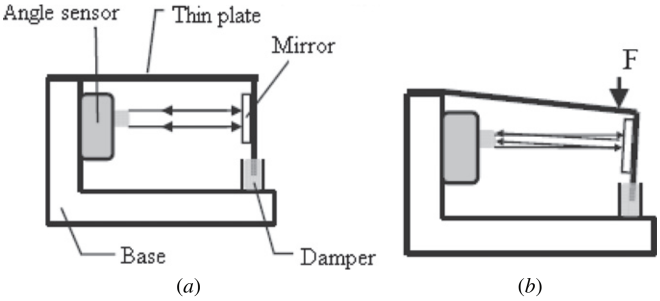

(*a*) (*b*)

Figure 9. Force sensor: (*a*) schematic diagram, (*b*) under loading condition.

3.2. Contact force calibration

A very sensitive force measurement apparatus has been designed and its schematic diagram is shown in figure 9(*a*). A thin leaf plate is built at the base. When a small force is applied to its end, a bending angle can be detected by an angular sensor, which is made from a DVD pickup head based on the autocollimator principle as shown in figure 9(*b*). This force sensor has been calibrated by some known weights and its linear force to the voltage range is about 200 μN. In the experiment, a microscope CCD is used to control the velocity of the probe contact, as shown in figure 10(*a*). Choosing various contact points of the probe ball in the same plane along corresponding normal directions, the corresponding contact force can be measured. In this experiment the force sensor was carried by the moving stage and driven by the HR4 in the GATE mode. Calibration results are shown in figure 10(*b*). It can be seen that the forces are mostly balanced in the horizontal *XY* plane. The average contact force calibrated in the *XY* plane is quite symmetrical, about 109 μN. Since the *Z*-stage of the micro-CMM has not been developed well enough, contact forces other than in this plane still show a certain degree of variation.

Table 3. Unidirectional touch-trigger repeatability experimental results.

Time	1	2	3	4	5	6	7	8	9	10	σ
Displacement (μm)	6.227	6.225	6. 218	6.225	6.245	6.232	6.219	6.220	6.229	6.240	8.9 nm

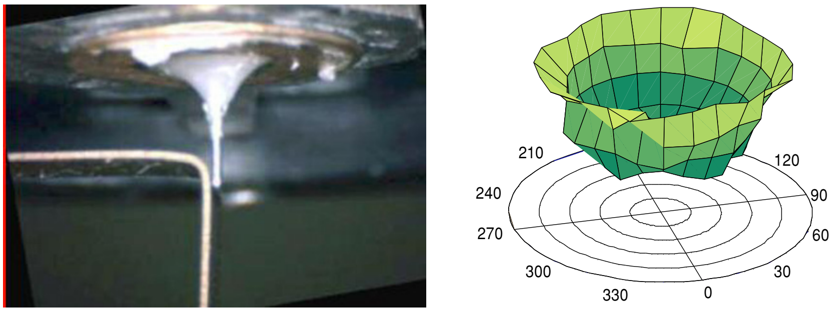

(*a*) (*b*)

Figure 10. Contact force calibration: (*a*) photo of the experiment, (*b*) 3D force plot.

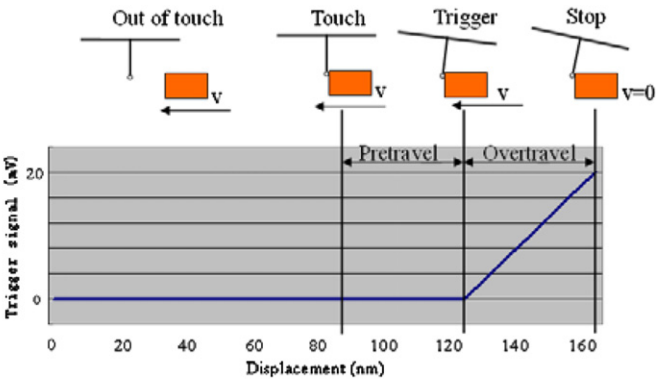

Figure 11. The output signals before and after a contact.

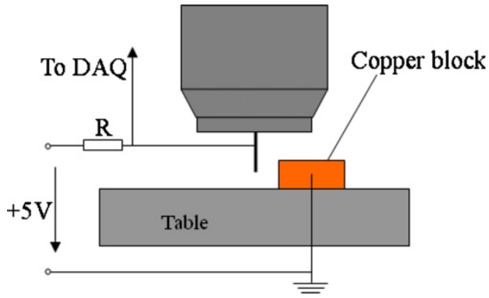

Figure 12. Touch point detection circuit.

3.3. Contact displacement calibration

At the moment of a touch, the double-trigger and the analog motion of the probe relative to the measured part are different, as shown in figure 11. Before the contact, the probe is at rest with no output signals from the focus sensors. The trigger point is determined as the time when the sensors detect the tilt motion of the floating plate. The distance between the touch and the trigger points is called the pre-travel distance, and the distance after the trigger point is called the overtravel or the scanning distance. Within the scanning range, the sensor output signal is linear with respect to the displacement. The trigger point is the intersection of two straight lines. The touch point can be detected by an on/off circuit as described in figure 12. The actual displacement can be calibrated by a laser interferometer.

The resulting displacements after repeating this program ten times are listed in table 3. The calculated standard deviation is 8.9 nm.

3.4. Pre-travel distance calibration

The double-trigger method has also been used for pre-travel distance calibration. The original distance of the probe before the touch point is reached can roughly be estimated. First, the ac mode is used to drive the moving stage that carries the workpiece to approach the probe. When the distance is approximately smaller than 0.5 mm, which is manually checked by using a microscope CCD as used in figure 10, the motion control is switched to the GATE mode. When the probe is touched by the workpiece, the sensing system is triggered for the first time. The GATE mode driving causes an overtravel of less than 50 nm. Then the stage is driven backward by about 200 nm in the GATE mode, and the trigger signal resumes the original level. Finally, the dc mode moves 200 nm forward, again with a very low speed of 10 nm s^{-1}, while the sensing system is triggered again and the triggered position is recorded. This double-trigger process is described by the flow chart in figure 13.

Figure 14 shows the data processing for the pre-travel distance calibration. The trigger point cannot be determined directly when noise is considered. To solve this problem, the lines before and after the trigger interval are best fitted by the least-squares method and the resulting intersection point defines the trigger position. Meanwhile, the step response of the touch signal is detected by the on/off signal described in figure 12. The pre-travel distance can thus be found.

To test the proposed method, the touch point and the trigger point are measured five times. The repeatability of

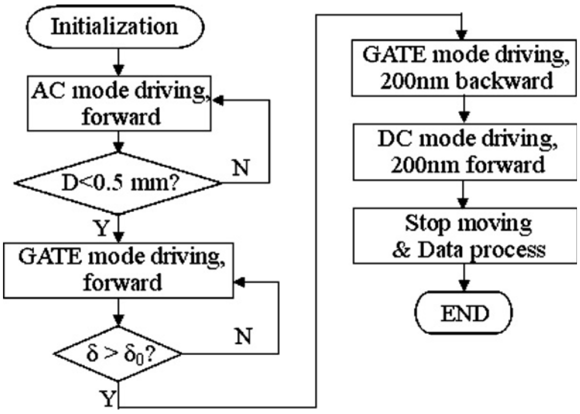

Figure 13. Double-trigger process (D: distance between the probe and the touch point; δ: signal voltage change; δ_0: threshold set for δ).

Table 4. Results of the pre-travel distance calibration.

Touch point (mm)	Trigger point (mm)	Pre-travel distance (nm)
1.102 387	1.102 397	10
1.102 399	1.102 405	6
1.102 376	1.102 389	13
1.102 380	1.102 390	10
1.102 395	1.102 406	11
σ = 10 nm	σ = 8 nm	Ave = 10 nm, σ = 2.5 nm

the experimental data as shown in table 4 demonstrates the reliability of this double-trigger method.

Figure 15 shows a plot of the pre-travel distances along eight directions in the XY plane. The pre-travel distance is quite symmetrical with an average value of 11 nm and the variation is about 1 nm. It proves that the floating mechanism of the probe system is feasible.

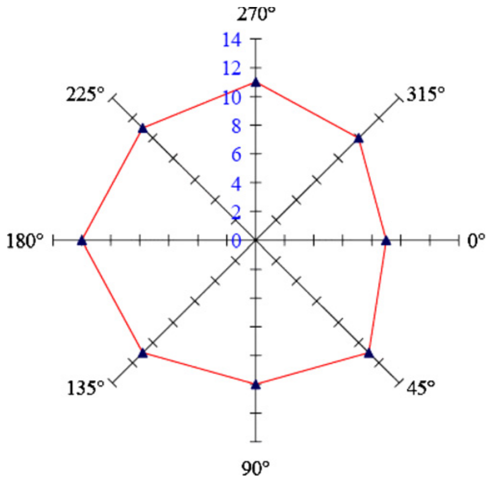

Figure 15. Pre-travel distances in the XY plane.

4. Conclusions

This paper describes the design of a touch scanning probe for a micro-CMM. This innovative probe combines a probe stylus, a mechanical floating mechanism and optical detectors, resulting in a high resolution with low cost. A novel suspension mechanism is proposed to increase the sensitivity and the stiffness of the structure has been calculated by the elasticity theory. A fine fiber probe tip has been developed to substitute the traditional ruby ball and the fabrication process has been optimized by using Taguchi's method, which guarantees both the roundness and the offset of the ball to be less than 1 μm. Experimental results show that the probe has a symmetrical contact force property in the horizontal XY plane. The contact force is found to be about 109 μN. The standard deviation of the unidirectional touch is less than 10 nm and the pre-travel distance is about 10 nm with a standard deviation of 3 nm. Such a scanning contact probe can measure

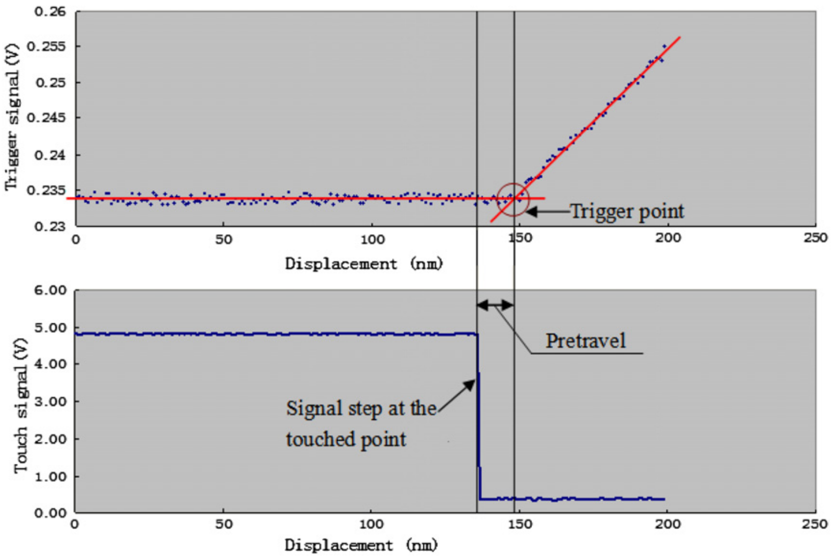

Figure 14. Signals for trigger-scanned points (top) and touch point (bottom) detection.

sidewalls and profile variation with nanometer resolution. The current stiffness is not balanced in all directions. Although adjusting the stylus length is a quick solution according to equation (2), it, however, also affects the pre-travel distance as well as the sensitivity of the probe. Future works will improve the capability in the Z-direction and the balance design of the stiffness.

Acknowledgments

The work reported is a part of a research program funded by the Natural Science Foundation of China (50420120134) and the National Science Council of Taiwan.

References

[1] McKeown P 1998 Nanotechnology-special article *Proc. Nano-Metrology in Precision Engineering (Hong Kong, 24–25 November 1998)* pp 5–55

[2] Fan K C *et al* 2006 Development of a low cost micro-CMM for 3D micro/nano measurements *Meas. Sci. Technol.* **17** 524–32

[3] Takamasu K, Furutani R and Ozono S 1997 Development of nano-CMM (coordinate measuring machine with nanometer resolution) *Proc. XIV IMEKO World Congress (Finland)* pp 34–9

[4] Peggs G N, Lewis A J and Oldfield S 1999 Design for a compact high-accuracy CMM *CIRP Ann.* **48** 417–20

[5] Haitjema H, Pril W O and Schellekens P 2001 Development of a silicon-based nanoprobe system for 3D measurements *CIRP Ann.* **50** 365–8

[6] Küng A, Meli F and Thalmann R 2007 Ultraprecision micro-CMM using a low force 3D touch probe *Meas. Sci. Technol.* **18** 319–27

[7] Chu C L and Chiu C Y 2007 Development of a low cost nanoscale touch trigger probe based on two commercial DVD pick-up heads *Meas. Sci. Technol.* **18** 1831–42

[8] Weckenmann A, Peggs G and Hoffmann J 2006 Probing systems for dimensional micro- and nano-metrology *Meas. Sci. Technol.* **17** 504–9

[9] Fan K C *et al* 2006 Experimental study of fabricating a micro ball tip on the optical fiber *J. Opt. A: Pure Appl. Opt.* **8** 782–7

[10] Fan K C, Wang W L and Chiou H S 2008 Fabrication optimization of a micro-spherical fiber probe with the Taguchi method *J. Micromech. Microeng.* **18** 0150111

[11] Ji H, Hsu H-Y, Kong L X and Wedding A B 2009 Development of a contact probe incorporating a Bragg grating strain sensor for nano coordinate measuring machines *Meas. Sci. Technol.* **20** 095304

[12] Fan K C, Lin C Y and Shyu L H 2000 The development of a low-cost focusing probe for profile measurement *Meas. Sci. Technol.* **11** N1–7

[13] Fan K C, Jäger G, Chen Y J and Mastylo R 2007 Development of a non-contact optical focus probe with nanometer accuracy *Proc. 7th Int. Conf. of EUSPEN (Bremen, Germany, 20–24 May 2007)* pp 278–81

[14] Hermann G 1983 Process intermittent measurement of tools and workpieces *J. Manuf. Syst.* **4** 41–9

[15] Fan K C, Ke Z Y and Li B K 2009 Design of a novel low-cost and long-stroke co-planar stage for nanopositioning *Tech. Mess.* **76** 248–52

[16] Chu C L, Fan K C and Chen Y J 2004 Design of a digital controller for long-stroke submicron positioning stage *Proc. 1st Int. Conf. of Positioning Technology (Act-city, Hamamatsu, Japan, 9–11 June 2004)* pp 176–81

[17] Fan K C and Cheng F 2006 Nanopositioning control on a commercial linear stage by software error correction *Nanotechnol. Precis. Eng.* **4** 1–9